

## Induced sensitivity of *Bacillus subtilis* colony morphology to mechanical media compression

Bacteria from several taxa, including *Kurthia zopfii*, *Myxococcus xanthus*, and *Bacillus mycooides*, have been reported to align growth of their colonies to small features on the surface of solid media, including anisotropies created by compression. While the function of this phenomenon is unclear, it may help organisms navigate on solid phases, such as soil. The origin of this behavior is also unknown: it may be biological (that is, dependent on components that sense the environment and regulate growth accordingly) or merely physical. Here we show that *B. subtilis*, an organism which typically does not respond to media compression, can be induced to do so with two simple and synergistic perturbations: a mutation that maintains cells in the swarming (chained) state, and the addition of EDTA to the growth media, which further increases chain length. EDTA apparently increases cell length by inducing defects in cell separation, as the treatment has only marginal effects on the length of individual cells. These results lead us to three conclusions. First, the wealth of genetic tools available to *B. subtilis* will provide a genetically tractable chassis for engineering compression sensitive organisms in the future. Second, the sensitivity of colony morphology to media compression in *Bacillus* is a physical rather than biological phenomenon dependent on a simple physical property of rod-shaped cells. And third, colony morphology under compression holds promise as a rapid, simple, and low-cost way to screen for changes in the length of rod-shaped cells or chains thereof.

# 1 Induced sensitivity of *Bacillus subtilis* colony morphology 2 to mechanical media compression

4 Jessica K. Polka<sup>1,2</sup> and Pamela A. Silver<sup>1,2\*</sup>

5 1. Systems Biology Department, Harvard Medical School

6 2. Wyss Institute for Biologically Inspired Engineering, Harvard University

7 \* To whom correspondence should be addressed

## 8 ABSTRACT

9 Bacteria from several taxa, including *Kurthia zopfii*, *Myxococcus xanthus*, and  
10 *Bacillus mycoides*, have been reported to align growth of their colonies to small  
11 features on the surface of solid media, including anisotropies created by  
12 compression. While the function of this phenomenon is unclear, it may help  
13 organisms navigate on solid phases, such as soil. The origin of this behavior is also  
14 unknown: it may be biological (that is, dependent on components that sense the  
15 environment and regulate growth accordingly) or merely physical.

16 Here we show that *B. subtilis*, an organism that typically does not respond to media  
17 compression, can be induced to do so with two simple and synergistic perturbations:  
18 a mutation that maintains cells in the swarming (chained) state, and the addition of  
19 EDTA to the growth media, which further increases chain length. EDTA apparently  
20 increases chain length by inducing defects in cell separation, as the treatment has  
21 only marginal effects on the length of individual cells.

22 These results lead us to three conclusions. First, the wealth of genetic tools available  
23 to *B. subtilis* will provide a new, tractable chassis for engineering compression  
24 sensitive organisms. Second, the sensitivity of colony morphology to media  
25 compression in *Bacillus* is a physical rather than biological phenomenon dependent  
26 on a simple physical property of rod-shaped cells. And third, colony morphology  
27 under compression holds promise as a rapid, simple, and low-cost way to screen for  
28 changes in the length of rod-shaped cells or chains thereof.

## 29 INTRODUCTION

30 Response of bacterial colony morphology (ie, orientation of growth) to small  
31 mechanical perturbations of growth media was first noted in *Kurthia*, a gram-positive  
32 genus notable for its striking feather-like morphology on gelatin slant cultures.  
33 (Sergent, 1906, 1907; Jacobsen, 1907; Stackebrandt, Keddie & Jones, 2006) A similar  
34 compression response has been reported in *Myxococcus xanthus*, where the  
35 phenomenon is dependent on adventurous motility, a flagellum- and pili-  
36 independent movement system.(Stanier, 1942; Fontes & Kaiser, 1999; Nan et al.,  
37 2014) Recently, the soil bacterium *Bacillus mycoides* was also shown to be sensitive  
38 to media perturbations.(Stratford, Woodley & Park, 2013) Interestingly, this  
39 compression response seems to occur by two different mechanisms: whereas  
40 individual *Myxococcus xanthus* dynamically reorients individual cells along lines of  
41 compression,(Dworkin, 1983) *Bacillus mycoides* instead gradually reorients the tips  
42 of chained cells as it grows.(Stratford et al., 2013)

43 The function of compression response is not known, but it has been suggested to aid  
44 navigation in natural environments on solid phases, like soil.(Dworkin, 1983) It has  
45 also been proposed as a potential tool for engineering applications in sensing  
46 environmental forces or generating patterns for nanofabrication.(Stratford et al.,  
47 2013)

48 Here we investigate whether increasing the length of chains of cells can induce  
49 compression sensitivity in an otherwise compression-insensitive species, *B. subtilis*.  
50 We employ a mutant of *B. subtilis* that forms long chains of cells (much like *B.*  
51 *mycoides*) and also deplete divalent cations in the media with EDTA;  $Mg^{2+}$  is thought  
52 be important for cell wall integrity. *B. subtilis* deprived of magnesium accumulates  
53 cell wall precursors.(Garrett, 1969) and magnesium is known to bind to components  
54 of the cell wall.(Heckels, Lambert & Baddiley, 1977) Notably, high magnesium  
55 concentrations can restore rod shape to cells with mutations in MreB, MreD, and  
56 PonA - all genes involved in cell wall synthesis.(Rogers, Thurman & Buxton, 1976;  
57 Rogers & Thurman, 1978; Murray, Popham & Setlow, 1998; Formstone & Errington,  
58 2005)

## 59 MATERIALS AND METHODS

### 60 Time lapse microscopy

61 2% LB agar was cut into approximately 10mm x 10mm squares and inoculated with  
62 1 $\mu$ l of liquid culture. The pad was then wedged, in a glass-bottomed dish (P35G-1.5-  
63 20-C, MatTek Corp.), between two plastic coverslips (Rinzi Plastic Coverslips, Size  
64 22x22mm, Electron Microscopy Science) manually bent in half at a 90° angle. Thus,  
65 half of each plastic coverslip made contact with the bottom of the dish, while the  
66 other half made contact with the agar pad. After placing a drop of approximately  
67 50 $\mu$ l of water on top of each plastic coverslip to maintain humidity in the dish, the  
68 MatTek dish was sealed with parafilm (this setup is illustrated in Fig. 1A). Cells were  
69 grown for approximately 6 hours at room temperature (approximately 23°) during a  
70 timelapse acquisition on a Nikon TE 2000 microscope equipped with an Orca ER  
71 camera, a 20x phase contrast objective, and Perfect Focus. A large area of the

72 sample was composited with automatic image stitching by Nikon Elements AR. Areas  
73 toward the center of the pad were selected for imaging.

#### 74 **Plate compression**

75 Microtiter format plates were prepared with LB + 2% agar. 24 hours after plates  
76 were poured, sterilized polystyrene spacers (each 0.080" thick, for a total  
77 compression of 0.16" or 4.1mm, equivalent to 4.8% compression) were inserted  
78 along the long dimension. Plates were stored at 37° for 24 hours, then inoculated  
79 from colonies grown on LB agar. Plates were incubated for 2-3 days at 30°, as the  
80 time required to reach colony dimensions >8mm varied with EDTA concentration.  
81 After incubation, plates were imaged with a gel imager and colony dimensions  
82 measured with FIJI.(Schindelin et al., 2012)

#### 83 **Cellular morphology**

84 Colonies were grown on LB + 2% agar containing either 0 or 125µM EDTA. After 24  
85 hours of incubation at 30°, cells from the edges of colonies were transferred directly  
86 to LB + 2% agar pads for imaging with the rounded bottoms of 0.6µl centrifuge  
87 tubes. To each pad, 1µl of an aqueous solution containing 10µg/ml FM4-64  
88 (Invitrogen) was added. Cells were imaged with a 100X phase contrast objective,  
89 and cell and chain lengths were measured manually with spline-fitted segmented  
90 lines in FIJI. Two-sample KS tests were performed.(Kirkman, 1996)

## 91 **RESULTS**

92 We first noted weak compression response of *B. subtilis* under the microscope.  
93 Unlike *B. mycooides*, *B. subtilis* colonies remain circular under compression under  
94 normal conditions. However, our microscopy assay (Fig. 1A) revealed that at small  
95 length scales (<100µm), *B. subtilis* cells display short-range alignment  
96 perpendicular to the direction of compression (marked with black arrows in Fig. 1A-  
97 C). Noting that the alignment is disrupted over longer length scales, we sought  
98 conditions under which *B. subtilis* cells might behave more similarly to *B. mycooides*.  
99 We noted that the chains of *B. subtilis* PY79 appeared shorter than that of *B.*  
100 *mycooides*, with the former reaching a maximum of approximately 300µm (Fig. 1C),  
101 while the can extend for millimeters(Stratford et al., 2013).

102 To increase chain length, we used *B. subtilis*  $\sigma^D::tet$ , a mutant that does not switch  
103 from swimming to swarming motility, and thus grows in long chains of cells (Kearns  
104 & Losick, 2005). To further perturb cell separation, we added EDTA to the growth  
105 medium.

106 To study colony morphology of *B. subtilis* under compression at the macroscopic  
107 scale with reproducible compression conditions, we prepared microtiter plates with  
108 LB + 2% agar and wedged polystyrene spacers between the agar and an edge of  
109 the plates (Fig. 2A). We inoculated the agar with colonies of *B. mycooides*, *B. subtilis*  
110 PY79, and *B. subtilis*  $\sigma^D::tet$ . Under 4.8% compression, *B. mycooides* forms elongated  
111 colonies as reported,(Stratford et al., 2013) while, without EDTA, *B. subtilis* colonies  
112 are round (Fig. 2A). With the addition of EDTA to the media, both *B. subtilis* PY79  
113 and  $\sigma^D::tet$  display a compression response (Fig. 2B). This is dependent on the

114 degree of compression; at 2.4% compression, both *B. subtilis* strains formed round  
115 colonies (data not shown).

116 We next quantified this effect over several colonies under each EDTA condition at  
117 4.8% compression. *Bacillus mycooides* forms colonies 4-4.5x larger in the dimension  
118 perpendicular to the direction of compression than parallel to it regardless of EDTA  
119 concentration (Fig. 2C). In comparison, the effect in *B. subtilis* is relatively small.  
120 *Bacillus subtilis* colonies were a maximum of approximately 1.5x larger in the  
121 direction perpendicular to compression, and this effect scaled with EDTA  
122 concentration (Fig. 2C). The EDTA effect was stronger for the  $\sigma^D::tet$  strain; at 125 $\mu$ M  
123 EDTA, compressed  $\sigma^D::tet$  colonies were 1.64x larger in the direction of compression  
124 (n=17, standard deviation 0.21), while PY79 colonies were 1.23x larger (n=16,  
125 standard deviation 0.20).

126 To understand how EDTA could affect compression response, we imaged cells taken  
127 directly from the edges of colonies on solid media containing either 0 $\mu$ M (Fig. 3A-C)  
128 or 125 $\mu$ M EDTA (Fig. 3D-F). The chains of *B. subtilis* cells, both PY79 and  $\sigma^D::tet$ , are  
129 longer on 125 $\mu$ M EDTA, but cell lengths, as delineated by the membrane dye FM4-  
130 64, are only marginally different. Quantification of ~300 chain and cell lengths for  
131 each strain under each condition (Fig. 4) reveals that *B. subtilis* chain lengths  
132 increase dramatically with the presence of EDTA, while *B. mycooides* chain lengths  
133 decrease slightly, suggesting that the EDTA effect on cell separation is specific to *B.*  
134 *subtilis* (Table 1).

## 135 DISCUSSION

136 These results suggest that the phenomenon of colony orientation under compression  
137 can be induced in the model organism *B. subtilis*. In contrast to *Bacillus mycooides*,  
138 the genetic tractability of *B. subtilis* will facilitate engineering of compression  
139 sensitive bacteria for use as environmental sensors or guides for nanofabrication.  
140 (Stratford et al., 2013)

141 Furthermore, the fact that that colony orientation on compressed media is  
142 generalizable indicates that it is likely to be a physical phenomenon. Rather than  
143 requiring biological components specific to *B. mycooides*, it is probably based on  
144 factors like rod length, stiffness, and tip vs. isotropic growth pattern.

145 Long rod length is a common feature of two prototypical compression responders,  
146 *Bacillus mycooides* and *Kurthia sp.*, which both grow as long chains of cells. (Di Franco  
147 et al., 2002; Stackebrandt et al., 2006) As seen in microscopy of *B. mycooides*, the  
148 absence of cell separation allows the bacteria to find and maintain a direction of  
149 compression. This same chaining property is responsible for the baroque colony  
150 morphology of *B. mycooides*: mutants that do not display this colony morphology  
151 have shorter chain lengths. (Di Franco et al., 2002) Thus, compression response may  
152 be driven by the same mechanisms that influence colony morphology under normal  
153 conditions; these mechanisms influence the manner in which cells explore and  
154 colonize their environment, and may be of critical importance in soil environments.

155 In the case of *B. subtilis*, the increase in compression sensitivity is based on chain  
156 length (as a  $\sigma^D$  mutant responds more than PY79, and both respond more strongly in  
157 the presence of EDTA, which also increases rod length). Though EDTA likely affects

158 multiple cellular processes, the role of  $Mg^{2+}$  in cell wall formation is clear.(Formstone  
159 & Errington, 2005) In particular, peptidoglycan hydrolases called autolysins are  
160 implicated in separation of cells after septation. Some of these autolysins, such as  
161 LytC, D, and F, are under the control of  $\sigma^D$ .(Chen et al., 2009) However, LytC  
162 expression can also be driven by  $\sigma^A$ .(Lazarevic et al., 1992) and this 50kDa amidase  
163 is activated by addition of  $Mg^{2+}$  *in vitro*.(Foster, 1992) This magnesium dependence  
164 of LytC and its regulation by a second sigma factor may explain why EDTA  
165 treatment further increases chain length in  $\sigma^D::tet$  cells. In addition to LytC, EDTA  
166 may be acting on other autolysins not regulated by  $\sigma^D$  (such as LytE or YwbG).  
167 (Smith, Blackman & Foster, 2000) The insensitivity of *B. mycooides* chain length to  
168 EDTA (Fig. 4, table 1) may be explained by species-specific differences in autolysins.

169 Inhibition of cell separation may not be the only relevant effect of EDTA, however.  
170 For example, perhaps depletion of  $Mg^{2+}$  changes the rigidity of cells such that they  
171 more readily align with the isotropic agar surface (Fig. 1B). An exhaustive  
172 understanding of EDTA's effects on the mechanical properties of *B. subtilis* walls  
173 remains to be attained.

174 The relatively weak maximal compression response we achieved with *B. subtilis*  
175 compared to *B. mycooides* suggests that other factors limit the compression response  
176 of *B. subtilis*. We suggest that one contributing factor is the growth pattern of this  
177 organism. Whereas *B. mycooides* elongates from its tips,(Turchi et al., 2012) *B.*  
178 *subtilis* inserts cell wall isotropically along its length.(Tiyanont et al., 2006) In  
179 micrographs of *B. subtilis* under compression, the chains of cells appear more  
180 buckled than those of *B. mycooides* (Fig. 1C); perhaps friction prevents the distal  
181 ends of the chain from sliding along to accommodate new growth from the middle of  
182 the chain. This buckling disrupts adjacent chains and is likely to lead to a more  
183 disorganized colony morphology. In the future, further modifications, perhaps  
184 increasing surfactin production, may increase the magnitude of this response.

185 Finally, because *B. subtilis* compression response depends on chain length, we  
186 propose that under some circumstances, colony morphology under compression  
187 could serve as a simple, high-throughput assay for perturbations to bacterial cell  
188 length and chain formation.

## 189 ACKNOWLEDGEMENTS

190 We thank Ethan Garner (Harvard University), Michael Baym (Harvard Medical School)  
191 and Ariel Amir (Harvard University) for helpful discussions. We are grateful to  
192 Stephanie Hays (Harvard Medical School) for critical reading of the manuscript.

## 193 REFERENCES

- 194 Chen R, Guttenplan SB, Blair KM, Kearns DB. 2009. Role of the  $\sigma^D$ -Dependent  
195 Autolysins in *Bacillus subtilis* Population Heterogeneity. *Journal of Bacteriology*  
196 191:5775–5784.

- 197 Dworkin M. 1983. Tactic behavior of *Myxococcus xanthus*. *Journal of Bacteriology*  
198 154:452–459.
- 199 Fontes M, Kaiser D. 1999. *Myxococcus* cells respond to elastic forces in their  
200 substrate. *Proceedings of the National Academy of Sciences* 96:8052–8057.
- 201 Formstone A, Errington J. 2005. A magnesium-dependent mreB null mutant:  
202 implications for the role of mreB in *Bacillus subtilis*. *Molecular Microbiology*  
203 55:1646–1657.
- 204 Foster SJ. 1992. Analysis of the autolysins of *Bacillus subtilis* 168 during vegetative  
205 growth and differentiation by using renaturing polyacrylamide gel  
206 electrophoresis. *Journal of Bacteriology* 174:464–470.
- 207 Di Franco C, Beccari E, Santini T, Pisaneschi G, Tecce G. 2002. Colony shape as a  
208 genetic trait in the pattern-forming *Bacillus mycoides*. *BMC Microbiology* 2:33.
- 209 Garrett AJ. 1969. The effect of magnesium ion deprivation on the synthesis of  
210 mucopeptide and its precursors in *Bacillus subtilis*. *The Biochemical Journal*  
211 115:419–430.
- 212 Heckels JE, Lambert PA, Baddiley J. 1977. Binding of magnesium ions to cell walls of  
213 *Bacillus subtilis* W23 containing teichoic acid or teichuronic acid. *Biochemical*  
214 *Journal* 162:359–365.
- 215 Jacobsen H. 1907. Ueber einen richtenden Einfluss beim Wachstum gewisser  
216 Bakterien in Gelatine. *Zentr. Bakt. Parasitenk.* II:53–64.
- 217 Kearns DB, Losick R. 2005. Cell population heterogeneity during growth of *Bacillus*  
218 *subtilis*. *Genes & Development* 19:3083–3094.
- 219 Kirkman T. 1996. Statistics to use.
- 220 Lazarevic V, Margot P, Soldo B, Karamata D. 1992. Sequencing and analysis of the  
221 *Bacillus subtilis* lytRABC divergon: A regulatory unit encompassing the  
222 structural genes of the N-acetylmuramoyl-L-alanine amidase and its modifier.  
223 *Journal of General Microbiology* 138:1949–1961.

- 224 Murray T, Popham DL, Setlow P. 1998. Bacillus subtilis cells lacking penicillin-binding  
225 protein 1 require increased levels of divalent cations for growth. *Journal of*  
226 *Bacteriology* 180:4555–4563.
- 227 Nan B, McBride MJ, Chen J, Zusman DR, Oster G. 2014. Bacteria that Glide with  
228 Helical Tracks. *Current Biology* 24:R169–R173.
- 229 Rogers HJ, Thurman PF. 1978. Temperature-sensitive nature of the rodB maturation  
230 in Bacillus subtilis. *Journal of Bacteriology* 133:298–305.
- 231 Rogers HJ, Thurman PF, Buxton RS. 1976. Magnesium and anion requirements of  
232 rodB mutants of Bacillus subtilis. *Journal of Bacteriology* 125:556–564.
- 233 Schindelin J, Arganda-Carreras I, Frise E, Kaynig V, Longair M, Pietzsch T, Preibisch S,  
234 Rueden C, Saalfeld S, Schmid B et al. 2012. Fiji: an open-source platform for  
235 biological-image analysis. *Nature Methods* 9:676–682.
- 236 Sergent E. 1906. Des tropismes du “Bacterium zopfii” Kurth. Premiere note. *Ann.*  
237 *inst. Pasteur*:1005–1017.
- 238 Sergent E. 1907. Des tropismes du “Bacterium zopfii” Kurth. Deuxieme note. *Ann.*  
239 *inst. Pasteur*:842–850.
- 240 Smith TJ, Blackman SA, Foster SJ. 2000. Autolysins of Bacillus subtilis: multiple  
241 enzymes with multiple functions. *Microbiology* 146:249–262.
- 242 Stackebrandt E, Keddie RM, Jones D. 2006. The Genus Kurthia. In: Dr MDP, Falkow S,  
243 Rosenberg E, Schleifer K-H, Stackebrandt E eds. *The Prokaryotes*. Springer US,  
244 519–529.
- 245 Stanier RY. 1942. A Note on Elasticotaxis in Myxobacteria. *Journal of Bacteriology*  
246 44:405–412.
- 247 Stratford JP, Woodley MA, Park S. 2013. Variation in the Morphology of Bacillus  
248 mycoides Due to Applied Force and Substrate Structure. *PLoS ONE* 8:e81549.
- 249 Tiyanont K, Doan T, Lazarus MB, Fang X, Rudner DZ, Walker S. 2006. Imaging  
250 peptidoglycan biosynthesis in Bacillus subtilis with fluorescent antibiotics.

251 *Proceedings of the National Academy of Sciences of the United States of*  
252 *America* 103:11033-11038.

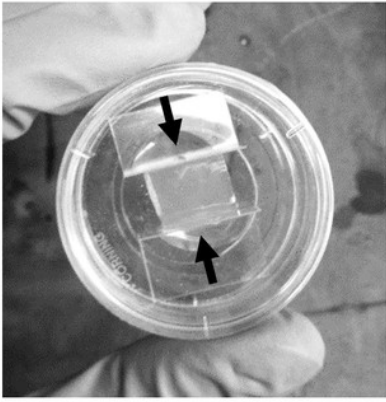
253 Turchi L, Santini T, Beccari E, Di Franco C. 2012. Localization of new peptidoglycan at  
254 poles in *Bacillus mycoides*, a member of the *Bacillus cereus* group. *Archives*  
255 *of Microbiology* 194:887-892.

# Figure 1

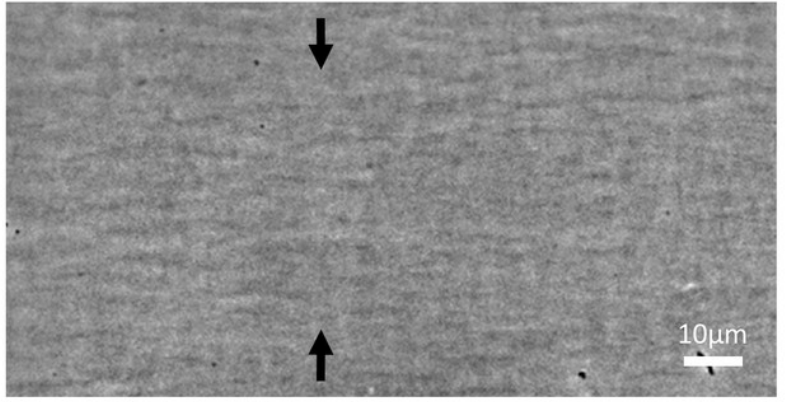
Microscopic morphology of *B. mycooides* and *B. subtilis* under compression.

A) Cells from liquid culture were applied to the bottom of an agarose pad compressed between plastic coverslips in a MatTek dish. Black arrows indicate direction of compression throughout. B) Striations visible in agar surfaces. C) Montages of timelapses of *B. mycooides*, *B. subtilis* PY79, and *B. subtilis*  $\sigma^D::tet$ . Note the striations visible in the agarose running perpendicular to the direction of compression.

A



B



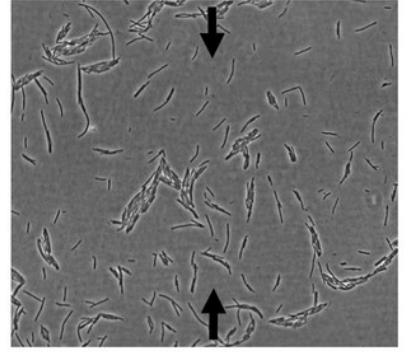
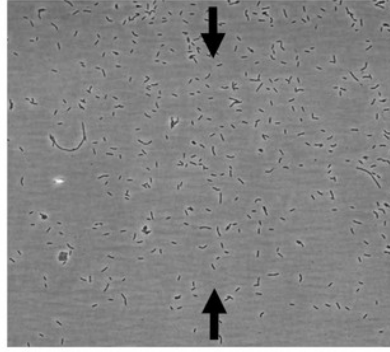
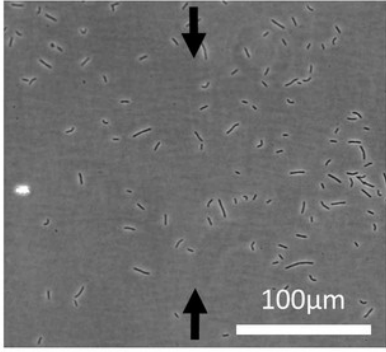
C

*B. mycooides*

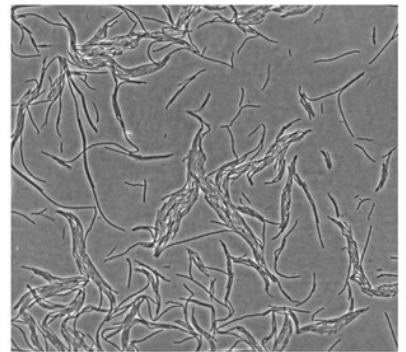
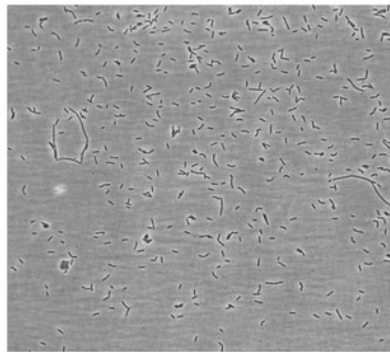
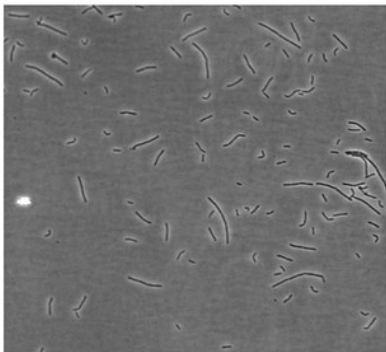
*B. subtilis* PY79

*B. subtilis*  $\sigma D::tet$

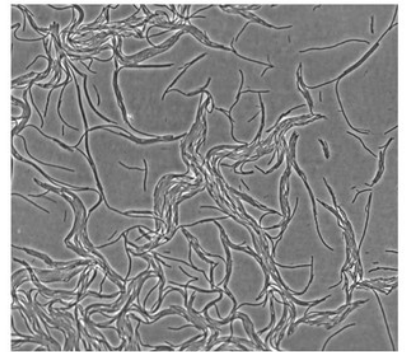
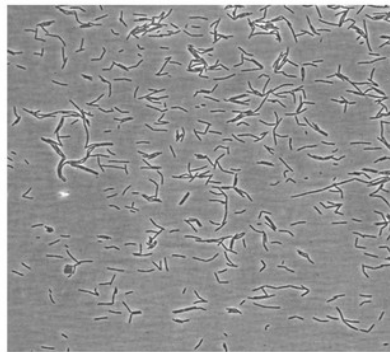
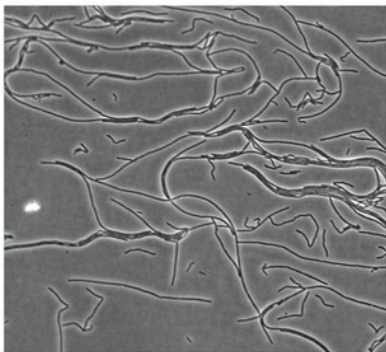
0 hrs



2 hrs



4 hrs



6 hrs

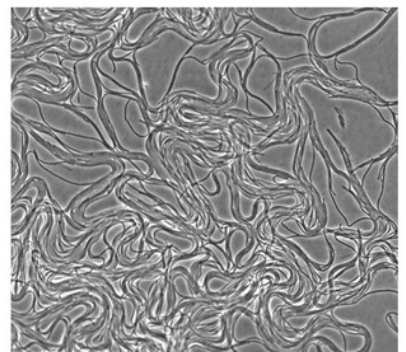
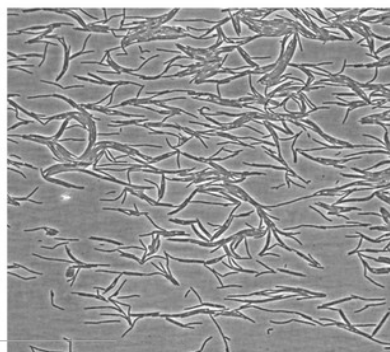
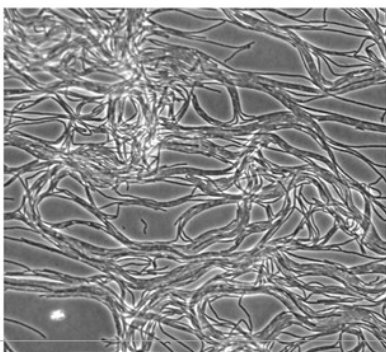


## Figure 2

*B. mycooides* and *B. subtilis* colony morphology under compression.

A) A microtiter plate inoculated with *B. mycooides* and *B. subtilis*. The two white bars at the top of the image of the plate are polystyrene spacers, totaling 4.8% of the plate height. Black arrows indicate direction of compression throughout. B) Representative images of *B. subtilis* PY79 and  $\sigma^D::tet$  colonies grown on compressed agar with varying EDTA concentrations. Scale bar, 1cm. C) Plot of colony shape ratio (ie, colony measurement perpendicular to the dimension of compression/colony measurement parallel to the dimension of compression) as it varies with EDTA concentration. D) Same as in C but with axes scaled to emphasize relative effect of PY79 and  $\sigma^D::tet$ . Source data for this figure can be found in supplementary dataset 1.

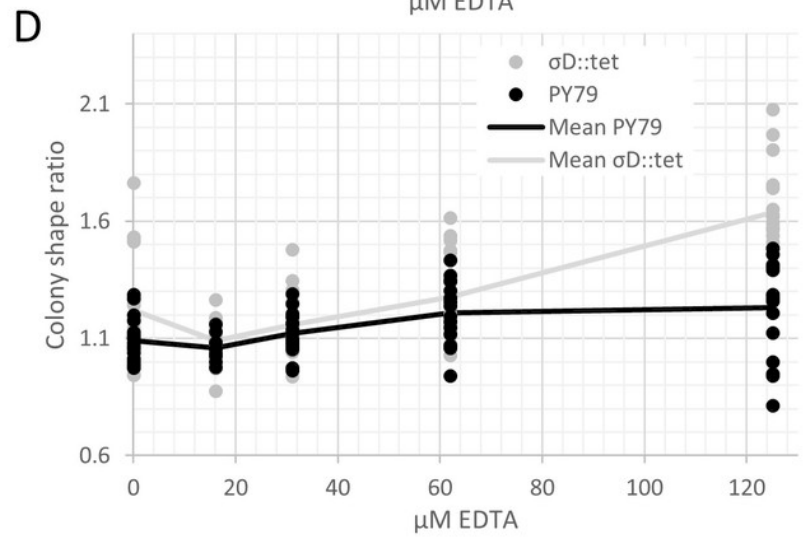
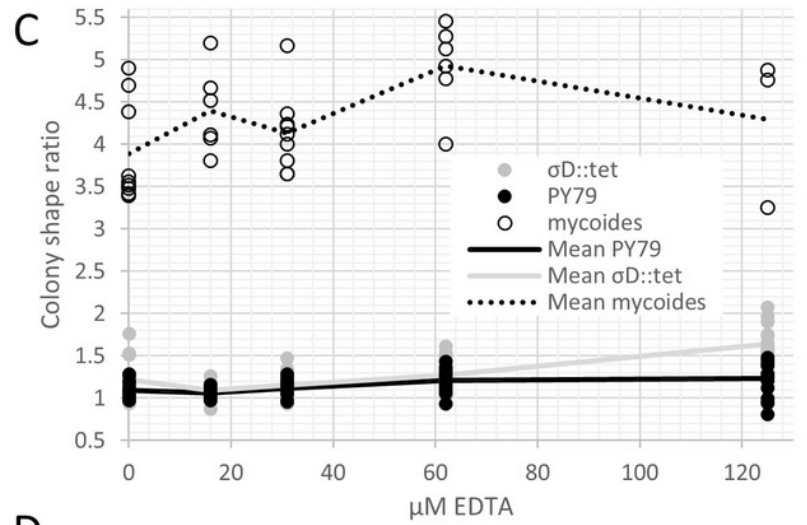
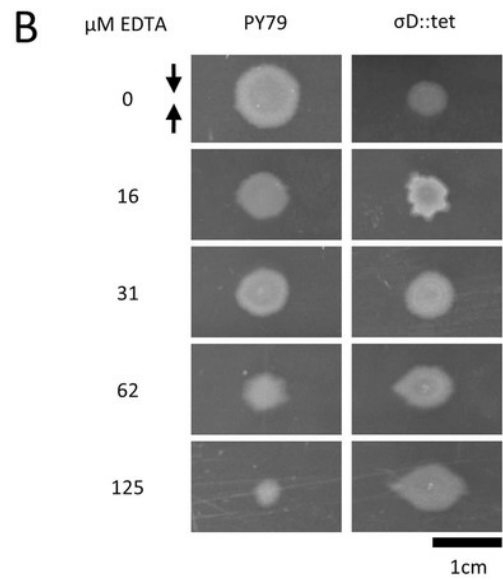
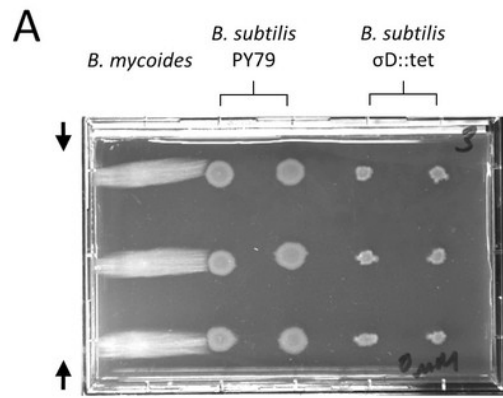


## Figure 3

Cellular morphology with and without EDTA.

A-C) *B. mycoides*, *B. subtilis* PY79, and *B. subtilis*  $\sigma^D::tet$ , respectively, growing on LB agar containing 0  $\mu$ M EDTA. D-F) As above on 125  $\mu$ M EDTA. In all images, phase contrast channel is in red, and FM4-64 is in green. Scale bar, 10  $\mu$ m. Source data for this figure can be found in supplementary dataset 2.

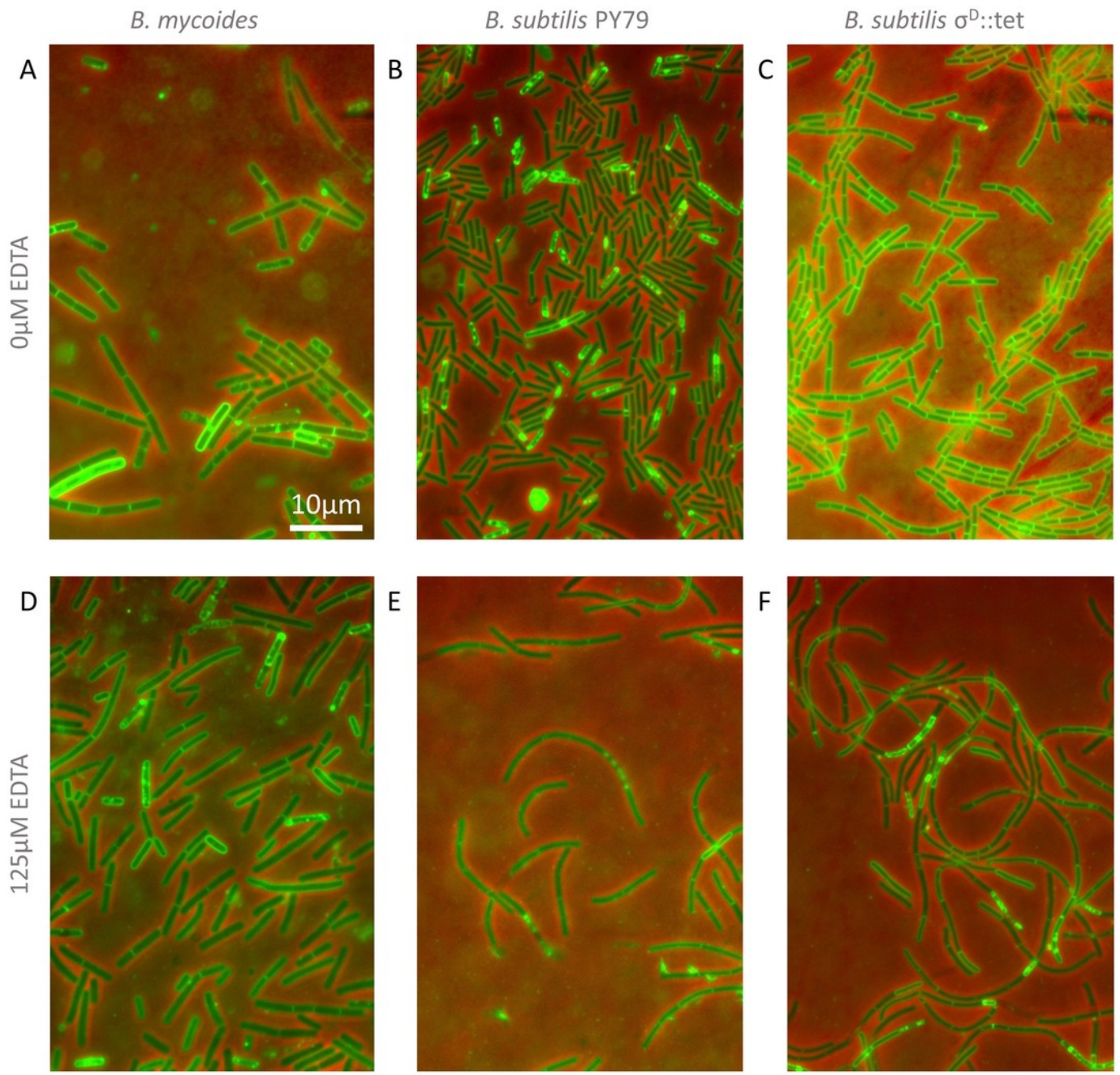


## Figure 4

Quantification of chain and cell lengths with and without EDTA.

A) Cell lengths of *B. mycooides* on 0 $\mu$ M (hollow bars) and 125 $\mu$ M EDTA (grey bars). B) Chain lengths of *B. mycooides*. C) Cell lengths of *B. subtilis* PY79. D) Chain lengths of *B. subtilis* PY79. E) Cell lengths of *B. subtilis*  $\sigma$ D::tet. F) Chain lengths of *B. subtilis*  $\sigma$ D::tet. Source data for this figure can be found in supplementary dataset 2.

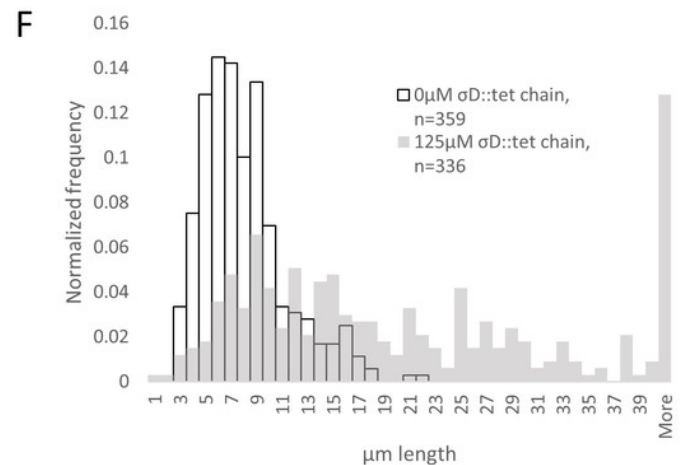
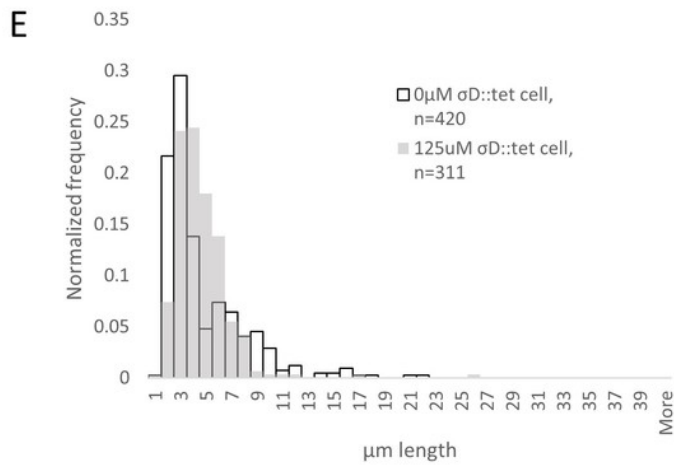
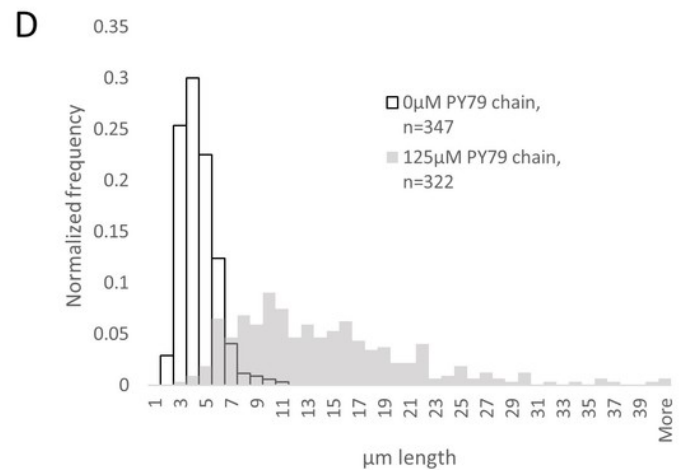
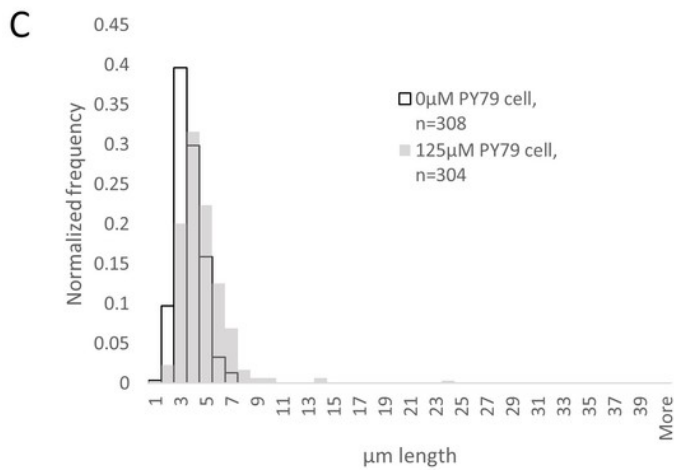
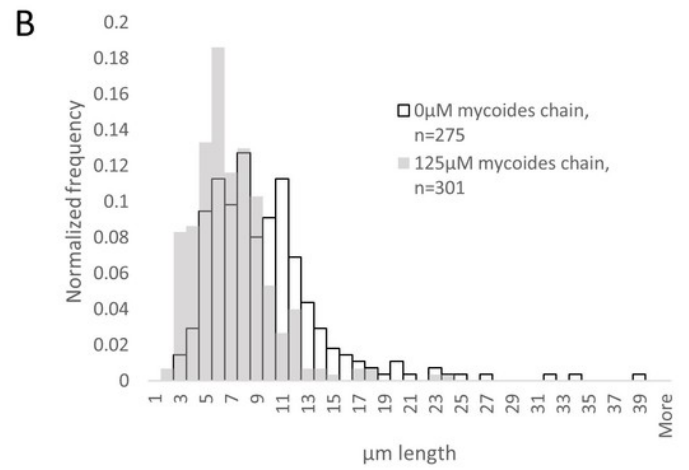
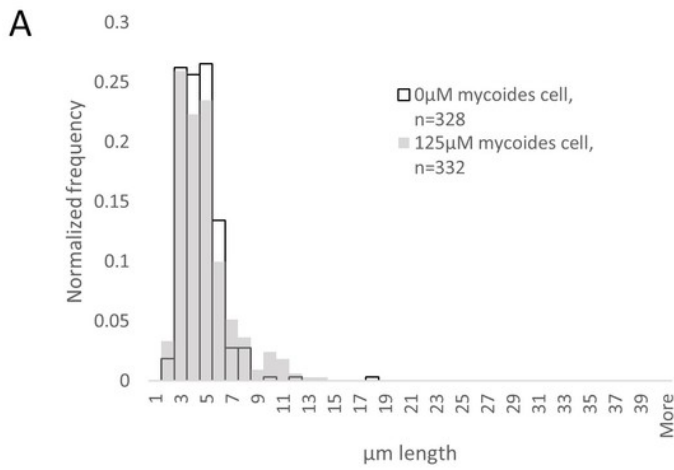


**Table 1** (on next page)

Properties of cell and chain length measurement distributions

**Table 1. Properties of cell and chain length measurement distributions**

	Cell length			Chain length		
	0 $\mu$ M EDTA mean ( $\mu$ m)	125 $\mu$ M EDTA mean ( $\mu$ m)	KS test maximum difference	0 $\mu$ M EDTA mean ( $\mu$ m)	125 $\mu$ M EDTA mean ( $\mu$ m)	KS test maximum difference
<i>B. mycoides</i>	4.01 (st dev 1.54)	4.33 (st dev 2.04)	D = 0.1044, P = 0.051	9.19 (st dev 4.81)	6.60 (st dev 3.09)	D = 0.2959, P = 0.000
<i>B. subtilis</i> PY79	3.18 (st dev 1.03)	4.18 (st dev 1.93)	D = 0.2866, P = 0.000	3.94 (st dev 1.38)	13.71 (st dev 7.23)	D = 0.8505, P = 0.000
<i>B. subtilis</i> $\sigma^D::tet$	4.23 (st dev 3.20)	4.12 (st dev 2.18)	D = 0.2413, P = 0.000	7.50 (st dev 3.36)	21.99 (st dev 18.1)	D = 0.5633, P = 0.000

**Table 2**(on next page)

Strains used in this study

**Table 2. Strains used in this study**

<b>Designation</b>	<b>Description</b>	<b>Reference</b>
<i>B. subtilis</i> PY79	Lab strain	Bacillus Genetic Stock Center 1A747
<i>B. subtilis</i> $\sigma^D::tet$	RL4169, DS323	Kearns and Losick, 2005 (Kearns & Losick, 2005)
<i>B. mycoides</i>		ATCC 6462